مجلة جامعة تشرين للبحوث والدراسات العلمية _ سلسلة العلوم الهندسية المجلد (31) العدد (5) 2009
Tishreen University Journal for Research and Scientific Studies - Engineering Sciences Series Vol. (31) No. (5) 2009

Analytical Modeling for the Precision Analysis of Angle Measurement System

Dr. Hasan Albustani*
Dr. Ali Ahmad**

(Received 21 / 10 / 2008. Accepted 12 / 2 / 2009)

□ ABSTRACT □

A two-sensor system based on the AMR effect is often used in automotive applications to compute the absolute angle of a steering-wheel. However, many possible errors may come from the sensors or from the signal conditioning electronics caused by the measurement errors or the input noise. These errors affect on the precision of the system. Thus, this demands on the precision analysis to determine whether the system delivers an accurate or correct output in the presence of the errors.

In this research, angular deviations caused by errors or noise will be modeled for the two sensor- system based on AMR sensors. Furthermore, the effect of the deviation on the precision of the system will be analyzed. MATLAB program is adopted for modeling, simulation, and evaluation of our results.

***Assistant Professor, Department of Communications and Electronics, Faculty of Mechanical and Electrical Engineering, Tishreen University, Lattakia, Syria**
****Associated Professor, Department of Communications and Electronics, Faculty of Mechanical and Electrical Engineering, Tishreen University, Lattakia, Syria**

مجلة جامعة تشرين للبحوث والدراسات العلمية _ سلسلة العلوم الهندسية المجلد (31) العدد (5) 2009
Tishreen University Journal for Research and Scientific Studies - Engineering Sciences Series Vol. (31) No. (5) 2009

النمذجة التحليلة من أجل تحليل الدقة لنظام قياس الزاوية

الدكتور حسن البستاني*[*]
الدكتور علي أحمد **[**]

(تاريخ الإيداع 21 / 10 / 2008. قُبِل للنشر في 2009/2/12)

□ ملخّص □

يستخدم نظام ثنائي الحساس الذي يعتمد على تأثير AMR في كثير من التطبيقات الخاصة بالسيارات لحساب الزاوية المطلقة α لدولاب القيادة. لكن العديد من الأخطاء الممكنة الحدوث في الحساسات أو في الكترونيات مكيفات الاشارة سببها أخطاء القياس أو ضجيج على دخل النظام. تؤثر هذه الاخطاء على دقة نظام القياس. لذلك لابد من تحليل الدقة لتحديد فيما اذا كان النظام سيعطي خرجاً دقيقاً أو صحيحاً بوجود هذه الأخطاء.

في هذا البحث سيتم نمذجة الانحرافات في الزاوية المطلقة α الناتجة عن الأخطاء أوالضجيج لنظام ثنائي الحساس الذي يعتمد على تأثير AMR. علاوة على ذلك سيتم تحليل تأثير الانحرافات على دقة النظام. يستخدم برنامج ال MATLAB من أجل نمذجة ومحاكاة وتقييم النتائج التي تمّ الحصول عليها.

[*] مدرس– قسم هندسة الاتصالات والالكترونيات– كلية الهندسة الميكانيكية والكهربائية– جامعة تشرين– اللاذقية
[**] أستاذ مساعد– قسم هندسة الاتصالات والالكترونيات– كلية الهندسة الميكانيكية والكهربائية– جامعة تشرين– اللاذقية

Introduction:

In automotive and other industrial applications an angle measurement is frequently required. The measuring system consists of the sensor and the signal processing subsystems as shown in Figure 1. The sensor converts the unknown quantity (e.g. angle) to be measured into an electrical signal that can be treated by a signal processing subsystem. The contactless angle measurement sensors such as magnetic sensors are often preferred because of their robustness against contamination and mechanical destruction. Moreover, the magnetic system and the signal conditioning electronics can be encapsulated separately. The magnetic sensors based on the anisotropic magneto-resistive (AMR) effect offer a good way to measure the angular position of the rotatable bodies. The AMR sensors are usually desired in automotive applications because of their robustness, precision and cost-efficiency.

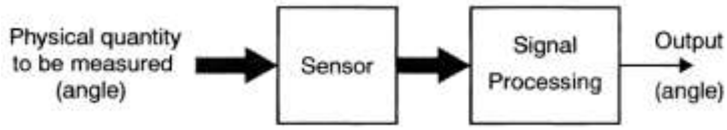

Figure 1: Angle measurement system

Objective of the Research:

The objective of the research can be described as follows:

- A two-sensor system based on the AMR effect is modeled to compute the absolute angle of a steering-wheel.
- Fault modeling is presented to model the maximum deviation of the input signals.
- Precision analysis is achieved to determine whether the system delivers an accurate or correct output in the presence of the errors.
- MATLAB program is used for modeling and simulation of our results.

Material and Research Method:

1- Steering-Wheel Angle Measurement Sensor

The steering-wheel angle measurement sensor was developed for using in automotive applications such as drive dynamic control systems (e.g. electronic stability program ESP). The system delivers the angle as an absolute value for the complete angular range of the steering column in bidirectional rotation. The angle of the steering column and the angular velocity are available at the output of the system via Controlled area Network (CAN) bus. The sensor gives the correct angle at the output immediately after switch-on without moving the steering column.

1-1- Measurement Principle

The steering-wheel drives two additional measuring gears by a main gear. A magnet is mounted on each measuring gear teeth. AMR sensors vary their resistances according to the magnetic field direction and deliver two sinusoidal signals. The microprocessor computes the angles after converting the analog signals into digital signals by using A/D converters as illustrated in Figure 2. The two measuring gears have different teeth numbers. Therefore, their relative angle and angular velocity are different. Both relative angles can be computed by **trigonometric functions**. Thus, the absolute angle of the steering-wheel is computed based on both relative angles.

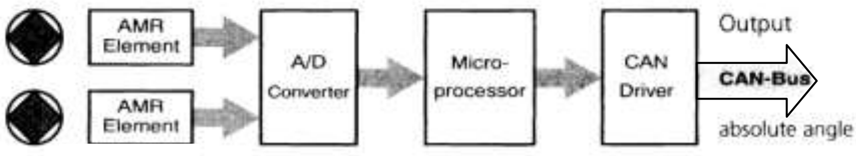

Figure 2: Measuring the absolute angle

1-2- Magneto-resistive Sensors

The magneto-resistive effect is the change of the electrical resistance of certain ferromagnetic material called permalloy due to an external magnetic field H [1]. The field H causes a rotation of the magnetization of the strip M. The resistance R of the permalloy strip depends on the angle α between the direction of electrical current I flowing through the strip and internal magnetization vector M. Thus, the resistance R of the ferromagnetic material changes as a function of the rotation angle α as given

$$R = R_0 + \Delta R_0 \cos^2 \alpha \qquad \textbf{(1-A)}$$

R_0 and ΔR_0 are material constants.

To achieve accurate measurements the internal magnetization vector M must directly follow the vector H of the external field. This can be achieved by applying an external field H much higher than the internal field M approximately 3 KA/m.

Philips Semiconductors provides a two-chip solution consisting of the magneto-resistive sensor KMZ41 or KMZ43 and the sensor signal conditioning IC UZZ9000 (analog output) and UZZ9001 (digital output) [1] [3] [4]. The magneto-resistive angle sensors of Philips Semiconductors are etched on a silicon substrate, with four permalloy strips arranged in a wheat-stone bridge configuration. The differential output signal $Vo(\alpha)$ ($+Vo(\alpha)$, $-Vo(\alpha)$) between both the voltage dividers of a Wheatstone bridge as shown in Figure 3 is

$$V_o = (V_{dd} - V_{ss})\left(\frac{R_3}{R_3 + R_1} - \frac{R_4}{R_4 + R_2}\right) \qquad \textbf{(1-B)}$$

According to the Eq.(1) and by considering the phases between the Wheatstone bridge resistances, the differential output signal (+Vo, -Vo) of a Wheatstone bridge is proportional to $\sin 2\alpha$.

$$V_o = (V_{dd} - V_{ss})\ K\ \sin 2\alpha \qquad \text{where K is a constant} \qquad \textbf{(1-C)}$$

The sensor based on one Wheatstone bridge can measure an angular range of 90° as shown in Figure 3 [3].

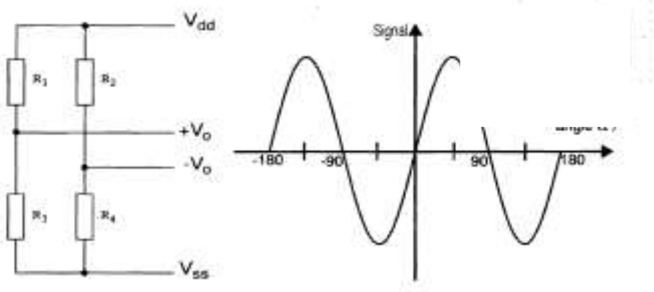

Figure 3: Wheatstone bridge and the sensor output signal

The output of the sensor depends on the temperature. Therefore, the temperature compensation should be added to avoid temperature effects. This can be achieved by using a two-bridge arrangement where the two bridges are positioned at an offset of 45° to each other as shown in Figure 4. The angular range becomes in this case 180°.

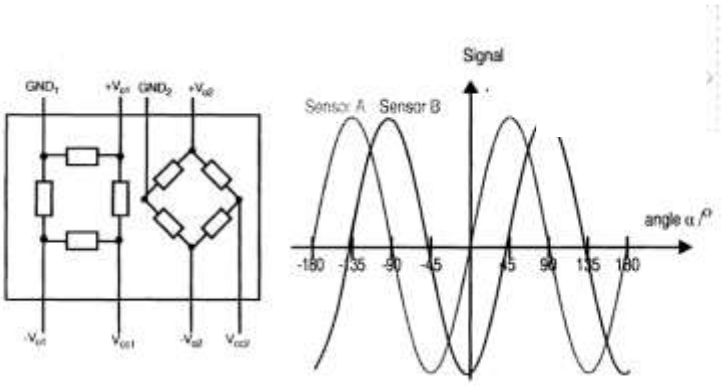

Figure 4: Double Wheatstone bridge sensor and output signals (KMZ41) [3]

The sensor provides two independent sinusoidal output signals which are 90° out of phase to each other. One of these signals is a function of sin2α and the other is a function of cos2α. The output signals can be described mathematically as follows:

$$x(\alpha, T) = X_0(T)\ \sin 2\alpha \quad (2)$$

$$y(\alpha, T) = Y_0(T)\ \cos 2\alpha \quad (3)$$

The requirement of the temperature measurement and the temperature compensation can be avoided if the amplitude of both signals are identical (xo = yo). Thus, the absolute angle α is:

$$\alpha = \frac{1}{2}\arctan\frac{x}{y} \quad (4)$$

1-3- The Two-Sensor System

The two-sensor system is depicted in Figure 5 [2]. A big gear with n teeth and two additional smaller gears with n_1 and n_2 teeth, respectively, are used whereas $n_1 > n_2$. The big gear rotates with an angle α and the smaller gears n_1, n_2 rotate with ψ and θ, respectively. The angles ψ and θ can be measured by using AMR sensors. The relationship between the angle α and ψ, θ can be described as follows:

$$\psi = \frac{n}{n_1}\alpha\,(\text{mod}\,\Omega) \qquad 0 \le \psi < \Omega \quad (5)$$

$$\theta = \frac{n}{n_2}\alpha\,(\text{mod}\,\Omega) \qquad 0 \le \theta < \Omega \quad (6)$$

(periodicity $\Omega = 180^{o}$) where mod is modulus operation

The equations (5), (6) are equivalent to

$$\alpha_i = \frac{n_1}{n}(\psi + i\ \Omega) \quad (7)$$

$$\alpha_j = \frac{n_2}{n}(\theta + j\ \Omega) \quad (8)$$

Where i, j are integer numbers

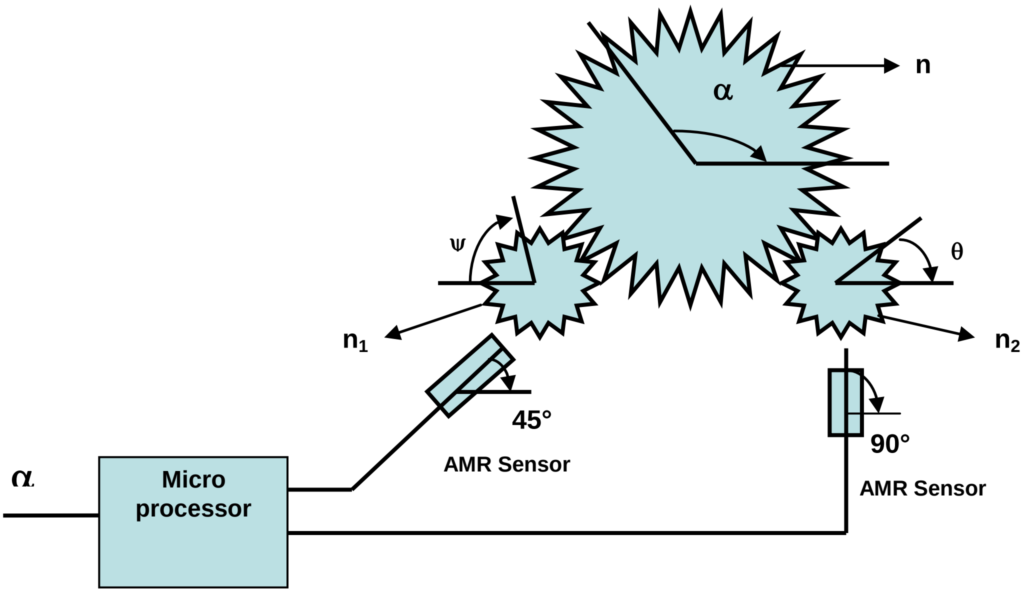

Figure 5 Angle measurements for a steering column using AMR sensors

It is $\alpha_i = \alpha_j$ thus

$$n_1\ i - n_2\ j = \frac{n_2\ \theta - n_1\ \psi}{\Omega} \tag{9}$$

Since the left-hand side of the equation is an integer number the right-hand side has also to be an integer number:

$$k = \frac{n_2\ \theta - n_1\ \psi}{\Omega} \tag{10}$$

Since both angles ψ and θ deviate from their nominal values, that means, k is a real number. Therefore, k must round up or down to the nearest integer. From Eq. (9) and (10) it yields to

$$n_1\ i - n_2\ j = k \tag{11}$$

This equation with two integer variables *i* and *j* has discrete solutions (first-order Diophantine equation) [5] [7]. From Eq.(10) the range of k is determined. The maximum value is obtained if ψ is 0° and θ is almost 180° thus $k < n_2$. In contrast, the minimum value is obtained if θ is 0° and ψ is almost Ω thus $k > -n_1$.

The Eq.(7) and (8) can be rewritten as follows:

$$\alpha_i = \frac{n_1}{n}\ \psi + \frac{n_1}{n}\ i\ \Omega$$

$$\alpha_j = \frac{n_2}{n}\ \theta + \frac{n_2}{n}\ j\ \Omega$$

The period of α is computed by this equation:

$$\text{period of } \alpha = \frac{n_1\ n_2}{n\ \gcd(n_1, n_2)}\ \Omega \quad , \tag{12}$$

(gcd = greatest common divisor)

The angles αi and αj range the complete absolute angle period if i = n2 and j = -n1. Assuming nl > n2, the ranges of k, i and j can be described as follows

$-n_1 < k < n_2 \qquad 0 \le i < n_2 \qquad 0 \le j < n_1 \qquad 0 \le i \le j$

To solve Eq. (11) three cases have to be considered:

a) n1 = n2 +1

For k ≥ 0, the solution is i = j = k

For k < 0, the solution is j = i + 1 and i = k + n2.

b) n1 > n2 + 1 and gcd(n1, n2) = 1: The Diophantine equation i n1 – j n2 = k is converted into congruence as follows:

$$n_1 \cdot i \equiv k (\bmod n_2) \qquad (13)$$

This congruence is solved by using the Gaussian trick [5]. The congruence in Eq. (13) is rewritten as

$$i \equiv \frac{k}{n_1} (\bmod n_2) \qquad (14)$$

Multiples of n2 are added or subtracted to k and n1 so that k/n1 becomes an integer.

***Example*: $(n, n_1, n_2) = (100, 37, 29)$.**

The Diophantine equation is $37\,i - 29\,j = k$.

Assuming that $k = 27$.

This equation is rewritten in congruence form

$$i \equiv \frac{27}{37} (\text{mod } 29)$$

The solutionis

$$i \equiv \frac{27}{37} \equiv \frac{27}{8} \equiv \frac{-2}{8} \equiv \frac{-1}{8} \equiv \frac{28}{4} \equiv 7 (\text{mod } 29)$$

$i = 7$, thus $j = 8$

c) if $\gcd(n_1, n_2) = c$, the Diophantine equation becomes

$$i\frac{n_1}{c} - j\frac{n_2}{c} = \frac{k}{c}$$

or

$$i\, n'_1 - j\, n'_2 = k' \qquad (15)$$

This equation can be solved as in (b)

2- Fault Modeling

There are some non-ideal cases affecting the precision of the system. These non-ideal cases are caused by different types of deviations in the system such as non-adequate magnetic field arrangements, non-ideal properties of sensors and non-ideal A/D transfer curves.

The signals xl, yl, x2 and y2 (see. Eq. (2) and (3)) may deviate from the nominal values by Δx1, Δy1, Δx2 and Δy2 respectively. The deviation in each channel is assumed to be independent of the other channels. The maximum deviation is assumed to be equal for all channels

$$\Delta x_{1max} = \Delta y_{1max} = \Delta x_{2max} = \Delta y_{2max} = \Delta xy$$

The precision of the system are evaluated as a function of the absolute angle α depending on this maximum deviation Δxy.

Figure 6 exhibits the complete block diagram for computing the absolute angle α. After switch-on, each sensor delivers two signals (x, y). The microprocessor computes ψ and θ by using the functions shown in Table 1. Then k is obtained by Eq.(10) and i, j by Eq.(11) or Eq. (15). αi and αj are computed by Eq.(7) and Eq.(8).

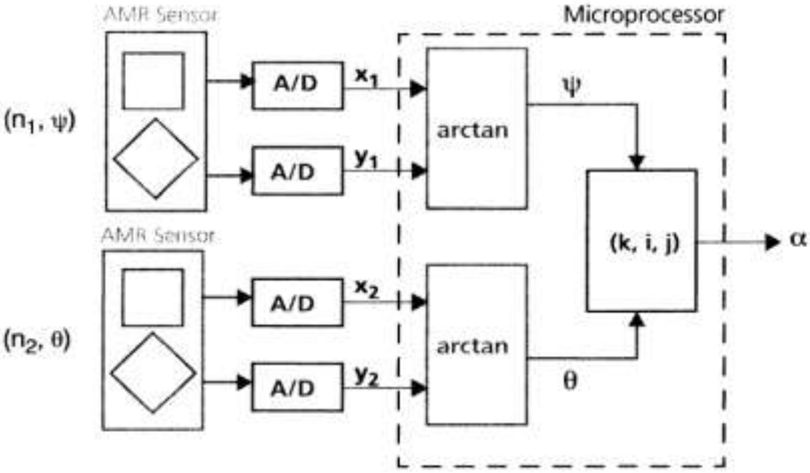

Figure 6: The complete block diagram for computing the absolute angle α

Table 1: Equations for computing ψ and θ corresponding to the range of input signals x and y

x	y	range of ψ or θ	ψ, θ
$0 \ldots \frac{\sqrt{2}}{2}$	$1 \ldots \frac{\sqrt{2}}{2}$	$0^o \ldots 22.5^o$	$\frac{1}{2}\arctan\frac{x}{y}$
			$\frac{1}{2}\arctan\frac{x}{y}$
$\frac{\sqrt{2}}{2} \ldots 1$	$\frac{\sqrt{2}}{2} \ldots 0$	$22.5^o \ldots 45^o$	$45° - \frac{1}{2}\arctan\frac{x}{y}$
$1 \ldots \frac{\sqrt{2}}{2}$	$0 \ldots -\frac{\sqrt{2}}{2}$	$45^o \ldots 67.5^o$	$\frac{1}{2}\arctan\frac{x}{y}$
$\frac{\sqrt{2}}{2} \ldots 0$	$-\frac{\sqrt{2}}{2} \ldots -1$	$67.5^o \ldots 90^o$	$90° + \frac{1}{2}\arctan\frac{x}{y}$
$0 \ldots -\frac{\sqrt{2}}{2}$	$-1 \ldots -\frac{\sqrt{2}}{2}$	$90^o \ldots 112.5^o$	$\frac{1}{2}\arctan\frac{x}{y}$
$-\frac{\sqrt{2}}{2} \ldots -1$	$-\frac{\sqrt{2}}{2} \ldots 0$	$112.5^o \ldots 135^o$	$135° - \frac{1}{2}\arctan\frac{x}{y}$
$-1 \ldots -\frac{\sqrt{2}}{2}$	$0 \ldots -\frac{\sqrt{2}}{2}$	$135^o \ldots 157.5^o$	$\frac{1}{2}\arctan\frac{x}{y}$
$-\frac{\sqrt{2}}{2} \ldots 0$	$\frac{\sqrt{2}}{2} \ldots 1$	$157.5^o \ldots 180^o$	$180° + \frac{1}{2}\arctan\frac{x}{y}$
			$\frac{1}{2}\arctan\frac{x}{y}$

3- Precision Analysis

From Eq.(7)and Eq.(8) α'i and α'j are calculated as follows:

$$\alpha'_i = \frac{n1}{n}(\psi' + i\ \Omega) \quad (16)$$

$$\alpha'_j = \frac{n2}{n}(\theta' + j\ \Omega) \quad (17)$$

The differences $\Delta\alpha i$ and $\Delta\alpha j$ are computed as:

$$\Delta\alpha_i = \alpha'_i - \alpha \quad (18)$$

$$\Delta\alpha_j = \alpha'_j - \alpha \quad (19)$$

The maximum deviation Δxy from the nominal values (x1, y1, x2, y2) leads to 9 values for ψ' and 9 values for θ'. That means, each $\Delta\alpha i$ and $\Delta\alpha j$ has also 9 values (cf. Eq.(18) and Eq.(19)). The maximum values of $\Delta\alpha_{imax}$ *and* $\Delta\alpha_{jmax}$ are selected. Thus, the precision of the system as a function of the absolute angle α ($\lambda = \lambda(\alpha)$) is determined by $\Delta\alpha_{imax}$ *and* $\Delta\alpha_{jmax}$ ($\lambda(\alpha) = |\Delta\alpha_{max}|$). Furthermore, the worst-case is defined as $\Lambda = \lambda(\alpha)_{max}|_{\Delta xy}$. From Eq. (16) and Eq. (17) the maximum deviations $\Delta\psi_{max}$ and $\Delta\theta_{max}$ ($\Delta\psi = \psi' - \psi$ and $\Delta\theta = \theta' - \theta$) lead to the maximum deviations $\Delta\alpha_{imax}$ and $\Delta\alpha_{jmax}$, respectively. The deviations $\Delta\theta_{max}$ and $\Delta\psi_{max}$ depend on the ranges of the input signals (x1, y1 or x2, y2) as illustrated in Figure 7.

Examples: For the range I the deviation $\Delta\psi$ is maximum if $x'=x+\Delta xy$ and $y'=y-\Delta xy$.

For the range II the deviation $\Delta\psi$ is maximum if $x'=x-\Delta xy$ and $y'=y+\Delta xy$.

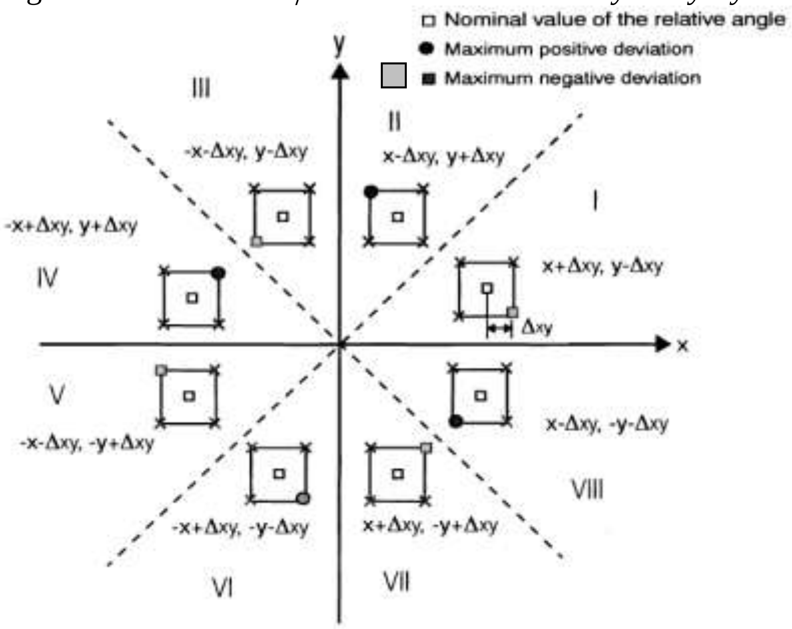

Figure 7: Maximum deviation of the relative angle corresponding to deviations of input signals

Simulation Results and Discussion:

1- Simulation Algorithm

The sinusoidal voltages (x1, y1), (x2, y2) are obtained as follows:

n, n1, n2, **Ω** are given and α_{max} is calculated according to Eq(12) (α_{max}=period of α).The angle α varies from 0° to α_{max}. For $\alpha = 0°$ and $\alpha = \alpha_{max}$ a small deviation makes the absolute angle belong to another period. Therefore, the absolute angle α is varied from $\alpha 0$

to α_{max}- $\alpha 0$. The $\alpha 0$ is a few degrees (2° or 3°) which guarantee that the absolute angle α belongs to the same period. It is assumed that the computed α_{max} (by Eq(12) must be greater than or equal to multiple of 360°. The input signals are computed as follows:

$$\varphi_1 = 2\ \alpha\ \frac{n}{n_1} \qquad \varphi_2 = 2\ \alpha\ \frac{n}{n_2}$$
$$x_1 = \sin\varphi_1 \qquad x_2 = \sin\varphi_2$$
$$y_1 = \cos\varphi_1 \qquad y_2 = \cos\varphi_2 \qquad (20)$$

Since the computation of the residue classes is time-consuming k, i and j are pre-computed in correspondence with Eq.(11) and stored in a look-up table. After calculating k. the corresponding i and j are fetched as shown in the second part of Table 2. The second column in Table 2 is range α|k.

In the following two examples are discussed for gcd (n1, n2) = 1 and gcd (n1, n2) = 2, respectively. The look-up tables for these examples are represented in Table 2 and Table 3. The values of n, n1, n2 and α for the first example are selected: n = 100, n1 = 37, n2= 29, Ω = 180°. The computed α_{max} is 800° as shown in Table 2. For the second example the given values are n= 42, n1= 28, n2= 26, **Ω=** 180.0°. The computed α_{max} is 1500° as shown in Table 3.

The simulation algorithm consists of the following steps:

1.Precompute k and corresponding i, jusing Eq. (11) and store them in look-up table.

2. Given α as the nominal value, the deviation Δxy.

3. Calculate the input signals using Eq. (20)

4. Compute ψ and θ by equations in Table 1, then k by Eq.(11).

5. Load i and j from look-up table (the second part of Table 2 and Table 3).

6. Compute (x'1, y'1, x'2, y'2)

7. Compute ψ' and θ' for the given deviation Δxy.

8. Compute $\alpha' i$ and $\alpha' j$

9. Compute $\Delta\alpha i$ and $\Delta\alpha j$ where $\Delta\alpha i = \alpha' i - \alpha$ and $\Delta\alpha j = \alpha' j - \alpha$

10. Determine max($|\Delta\alpha i|$) and max($|\Delta\alpha j|$)

The computation of the precision is illustrated in Figure 8. The precision as a function of αi ($\lambda = \lambda(\alpha i)|_{\Delta xy}$) nd a, ($\lambda = \lambda(\alpha j)|_{\Delta xy}$) are determined by max(Δαi) and max(Δαj), respectively.

As a result, the precision of αj is better than the precision of αi**.** Therefore, the output of the system is α*j* and the precision Λ of the system is equal to $\lambda(\alpha j)_{max}$ ($\Lambda = \lambda(\alpha j)_{max}$).

Table 2: k, i and j corresponding to the absolute angle α for (n, n1, n2) = (100, 37, 29) gcd(n1,n2) = 1, the second part presents the stored values in look-up table.

$\alpha/^o$	range $\alpha\|_k$	k	i	j
0.00	52.20	0	0	0
52.20	14.40	-29	0	1
66.60	37.80	8	1	1
104.40	28.80	-21	1	2
133.20	23.40	16	2	2
156.60	43.20	-13	2	3
199.80	9.00	24	3	3
208.80	52.20	-5	3	4
261.00	5.40	-34	3	5
266.40	46.80	3	4	5
313.20	19.80	-26	4	6
333.00	32.40	11	5	6
365.40	34.2	-18	5	7
399.60	18.00	19	6	7
417.60	48.60	-10	6	8
466.20	3.60	27	7	8
469.80	52.20	-2	7	9
522.00	10.80	-31	7	10
532.80	41.40	6	8	10
574.20	25.20	-23	8	11
599.40	27.00	14	9	11
626.40	39.60	-15	9	12
666.00	12.60	22	10	12
678.60	52.20	-7	10	13
730.80	1.80	-36	10	14
732.60	50.40	1	11	14
783.00	16.20	-28	11	15
799.20	36.00	9	12	15

k	i	j
-36	10	14
-35	21	28
-34	3	5
-33	14	19
-32	25	33
-31	7	10
-30	18	24
-29	0	1
-28	11	15
-27	22	29
-26	4	6
-25	15	20
-24	26	34
-23	8	11
-22	19	25
-21	1	2
-20	12	16
-19	23	30
-18	5	7
-17	16	21
-16	27	35
-15	9	12
-14	20	26
-13	2	3
-12	13	17
-11	24	31
-10	6	8
-9	17	22

Table 3: k, i and j corresponding to the absolute angle α for (n, n1, n2) = (42, 28, 26), gcd(n1,n2) = 2, the second part presents the stored values in look-up table.

α / °	range $\alpha\|_k$	k	i	j
0.00	111.43	0	0	0
111.43	8.57	-26	0	1
120.00	102.86	2	1	1
222.86	17.14	-24	1	2
240.00	94.29	4	2	2
334.28	25.71	-22	2	3
360.00	85.72	6	3	3
445.71	34.28	-20	3	4
480.00	77.14	8	4	4
557.14	42.86	-18	4	5
600.00	68.57	10	5	5
668.57	51.43	-16	5	6
720.00	60.00	12	6	6
780.00	60.00	-14	6	7
840.00	51.43	14	7	7
891.43	68.57	-12	7	8
960.00	42.86	16	8	8
1002.86	77.14	-10	8	9
1080.00	34.28	18	9	9
1114.28	85.72	-8	9	10
1200.00	25.71	20	10	10
1225.71	94.29	-6	10	11
1320.00	17.14	22	11	11
1337.14	102.86	-4	11	12
1440.00	8.57	24	12	12
1448.57	111.43	-2	12	13

k	i	j
-26	0	1
-24	1	2
-22	2	3
-20	3	4
-18	4	5
-16	5	6
-14	6	7
-12	7	8
-10	8	9
-8	9	10
-6	10	11
-4	11	12
-2	12	13
0	0	0
2	1	1
4	2	2
6	3	3
8	4	4
10	5	5
12	6	6
14	7	7
16	8	8
18	9	9
20	10	10
22	11	11
24	12	12

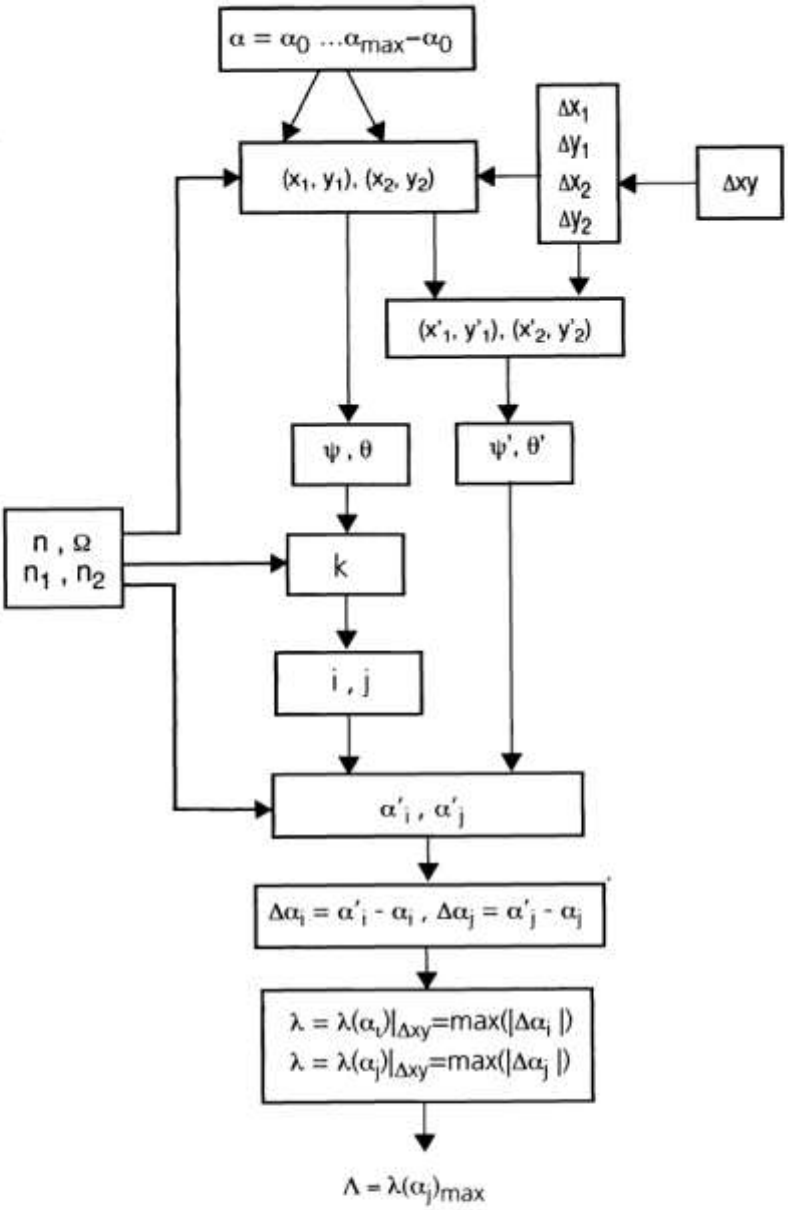

Figure 8: Block diagram for the computation of the precision

2- Results and Discussion

The precision of the system is determined by the maximum deviations $\Delta\alpha i$ and $\Delta\alpha j$. The precision as a function of the absolute angle α is defined by $\lambda = \lambda(\alpha j)\,|_{\Delta xy}$ with Δxy given the precision as a function of the absolute angle α is determined. The maximum and minimum deviation values (Δxy = 0.0693 and Δxy = 0.02) are selected as examples. Δxy = 0.02 is assumed for the first three examples (figure 9, 10, and 11) and Δxy = 0.0693 for the last example (figure 12). In figure 12, the distortion in the peaks of waves is caused by the switch between the ranges as mentioned in Table 1.

The results and the figures are obtained via MATLAB Tools [9]. The precision Λ of the system is equal to $\Delta\alpha j_{max}$. The computation results are given in Table 4.

Table 4: Precision computation results

	(n, n_1, n_2)	α_{max}	Δxy	$\Delta\alpha_{imax}$	$\Delta\alpha_{jmax}$	Λ
$n_1 = n_2 + 1$	(100,30,29)	1566^o	0.02	0.243^o	0.235^o	0.235^o
$n_1 > n_2 + 1$ gcd(n_1, n_2)=1	(100,37,29)	1931.4^o	0.02	0.300^o	0.235^o	0.235^o
$n_1 > n_2 + 1$ gcd(n_1, n_2)=2	(87,40,38)	1572.4^o	0.02	0.373^o	0.354^o	0.354^o
$n_1 > n_2 + 1$ gcd(n_1, n_2)=2	(42,28,26)	1560^o	0.0693	1.875^o	1.741^o	1.741^o

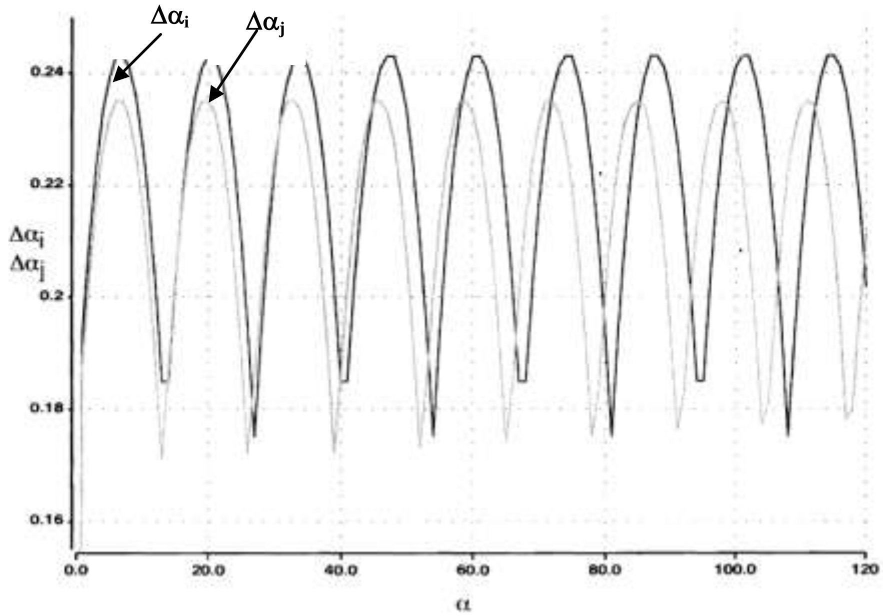

Figure 9: The accuracy $\lambda=\lambda(\alpha)$ for (n, n1, n2) = (100, 30, 29), Δxy = 0.02

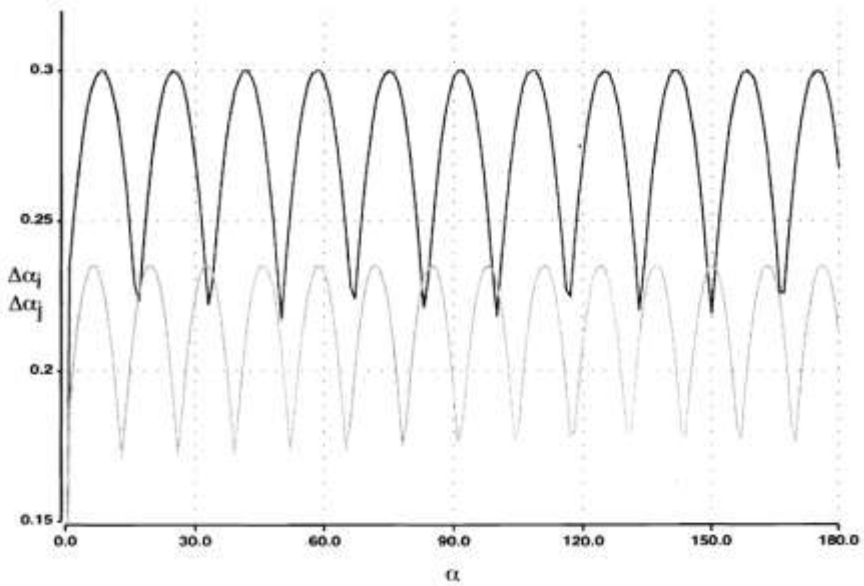

Figure 10: The accuracy $\lambda=\lambda(\alpha)$ for (n, n1, n2) = (100, 37, 29), Δxy = 0.02

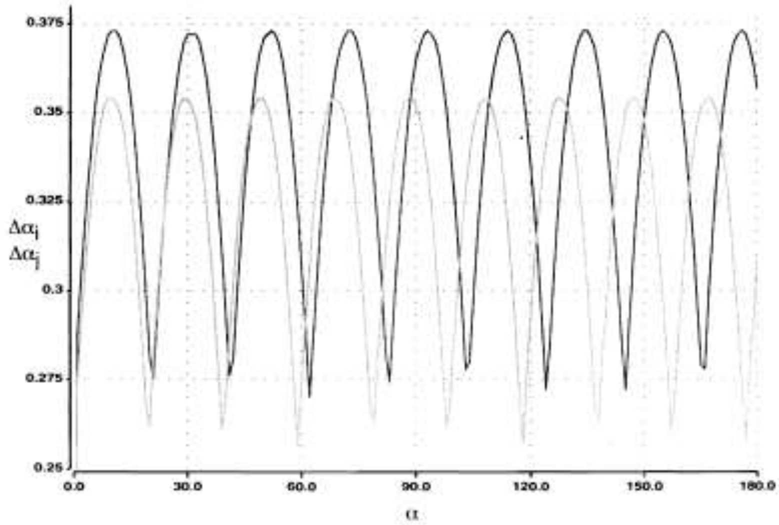

Figure 11: The accuracy $\lambda = \lambda\ (\alpha)$ for (n, n1, n2) = (87, 40,38), Δxy = 0.02

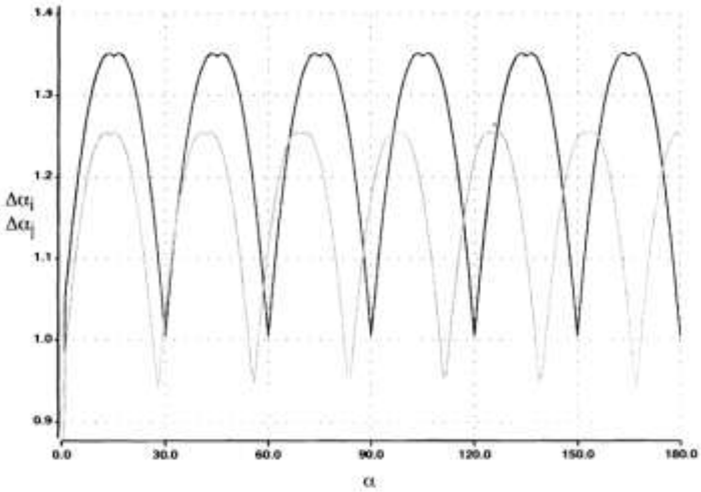

Figure 12: The accuracy $\lambda = \lambda\ (\alpha)$ for (n, n1, n2)= (42, 28, 26), Δxy = 0.0693

Conclusion and Recommendations:

In this research the absolute angle for the rotatable steering column was measured by using the two-sensor system. The precision have been modeled to determine whether the system delivers an accurate output. The precision Λ of the system is computed for a given deviation Δxy of voltages of the sensors. By means of simulation it could be concluded that *the best precision of α is achieved if the angle α of the smaller gear is taken*.

Finally, we can suggest the two recommendations as future works:

- Other sensor types can be used to measure the absolute angle for rotatable steering column.
- Multiple sensors can be used to obtain higher reliability of the measuring system.

References:

[1] DIETMAYER, K.; WESER M. *Contactless Angle Measurement using KMZ41 and UZZ9001*. Application Note AN00004, Philips Semiconductors, 17. January 2000.

[2] DILGER; E. *Vorrichtung und Verfahren zur Messung der Winkellage eines Drehbaren Korpers*, Patent DE 198 55 960 A 1. 15. Juni 2000.

[3] PHILIPS SEMICONDUCTORS *KMZ41 Magnetic field sensor*, *Objective specification*, *Data Sheet*, Philips Semiconductors, 18. April 2000.

[4] PHILIPS SEMICONDUCTORS *KMZ43*, *Magnetic field sensor*, *Objective specification*, *Data Sheet*, Philips Semiconductors, 24. August 2000.

[5] SCHROEDER; M. R. *Number theory in science and communication*. Springer Verlag, United States of America, 1997.

[6] DILGER, E.; GULBINS, M.; OHNESORGE, T.; STRAUBE B. *On a Redundant Diversified Steering Angle Sensor*. Proceedings of the 9th IEEE International On-Line Testing Symposium (IOLTS'03), 2003.

[7] BURTON, D. M. *Elementary Number Theory*. McGraw-Hill, New York, 2007.

[8] FRADEN, J. *Handbook of Modern Sensors: Physics, Designs, and Applications*. Springer Verlag, United States of America, 2004.

[9] www.mathworks.com, Access date 10/10/2007.